International Journal of Mass Spectrometry 279 (2009) 32–36

Contents lists available at ScienceDirect

International Journal of Mass Spectrometry

journal homepage: www.elsevier.com/locate/ijms

Collision-induced dissociation of protonated nanodroplets

Keri McQuinn, Fraser Hof*, J. Scott McIndoe**

Department of Chemistry, University of Victoria, P.O. Box 3065, Victoria, BC V8W 3V6, Canada

ARTICLE INFO

Article history:
Received 7 August 2008
Received in revised form
29 September 2008
Accepted 1 October 2008
Available online 17 October 2008

Keywords:
Water cluster
Nanodroplet
Electrospray ionization
Collision-induced dissociation
Magic number

ABSTRACT

Protonated nanodroplets are easily generated using electrospray ionization mass spectrometry (ESI–MS) and may be isolated and fragmented using collision-induced dissociation (CID), causing sequential loss of water molecules. These studies reveal not only the expected high stability of the "magic" protonated water cluster $[H(H_2O)_{21}]^+$, a dodecahedral clathrate cage, but also a new, rather more subtle trend in stabilities of product ions that manifests itself as increased stability of clusters that have a multiple of 12–13 water molecules.

1. Introduction

There is significant interest in solvent cluster research as a link between the gas phase and the solution phase. Water clusters are of particular interest because of the unique hydrogen bonding capabilities of water and its importance in chemistry and biology [1,2]. Protonated water clusters have been studied extensively for many years and are routinely used for calibration purposes in mass spectrometry; $[H(H_2O)_n]^+$ ions are produced readily and cover a large m/z range ($n = 1$ to >100) [3]. One of the main focuses of water cluster research has been on the "magic" $[H(H_2O)_{21}]^+$ cluster, first identified in 1973 by Lin [4], who observed through mass spectrometry experiments that water cluster intensities decreased as the number of water molecules increased with the exception of the 21-mer and the 22-mer where a discontinuity occurred. The $[H(H_2O)_{21}]^+$ ion had a larger intensity than expected while the $[H(H_2O)_{22}]^+$ cluster had a smaller intensity than expected. This $[H(H_2O)_{21}]^+$ cluster has been described as "magic" due to this anomalous intensity observed in many different mass spectrometry [5–9] experiments, indicating that it has a particularly stable structure. The $[H(H_2O)_{28}]^+$ cluster has also been observed to have special stability as a weak maximum is seen for the 28-mer in $[H(H_2O)_n]^+$ mass spectra [5–7,10]. The behaviour and existence of these magic number clusters are independent of the source of ionization. Many different techniques have been successful in generating these ensembles of water clusters including electrospray ionization (ESI) [3], electron impact ionization (EI) [10], corona-discharge ionization [11], chemical ionization (CI) [12], electrospray droplet impact [13] and femtosecond photoionization [2].

Searcy and Fenn suggested that the $[H(H_2O)_{21}]^+$ cluster had a pentagonal dodecahedral cage structure to account for its high stability [14]. The structure of a range of protonated water clusters has been probed through vibrational predissociation spectroscopy [11,15–17]. In these experiments $[H(H_2O)_n]^+$ are generated in an ion source, mass selected in a tandem mass spectrometer and excited using an infrared laser. The spectrum produced is dependent on the size and structure of the water cluster being investigated [15,17]. Shin and co-workers [15] report the O–H stretching vibrational spectra of $[H(H_2O)_n]^+$ clusters with $6 \leq n \leq 27$. The spectra of the $[H(H_2O)_{21}]^+$ and $[H(H_2O)_{22}]^+$ differ from their neighbouring clusters as they only show a single peak instead of a doublet, implying that *all* of the dangling OH groups on the $[H(H_2O)_{21}]^+$ cluster are due to water molecules that are bound in a similar way, providing support for the pentagonal dodecahedral cage structure.

The structure of $[H(H_2O)_{21}]^+$ has also been modeled by a variety of computational methods including ab initio calculations [18–21], Monte Carlo simulations [22–24], and molecular dynamics simulations [25]. These models also suggest that the stability of the $[H(H_2O)_{21}]^+$ cluster is due to a distorted pentagonal dodecahedral cage structure (Fig. 1). This structure is especially stable because each water molecule is hydrogen bonded to three other water molecules within the cage. There has been much debate as to what is found in the centre of the cage: a single water molecule or a

* Corresponding author.
** Corresponding author. Tel.: +1 250 721 7181; fax: +1 250 721 7147.
E-mail address: mcindoe@uvic.ca (J.S. McIndoe).

1387-3806/$ – see front matter © 2008 Elsevier B.V. All rights reserved.
doi:10.1016/j.ijms.2008.10.001

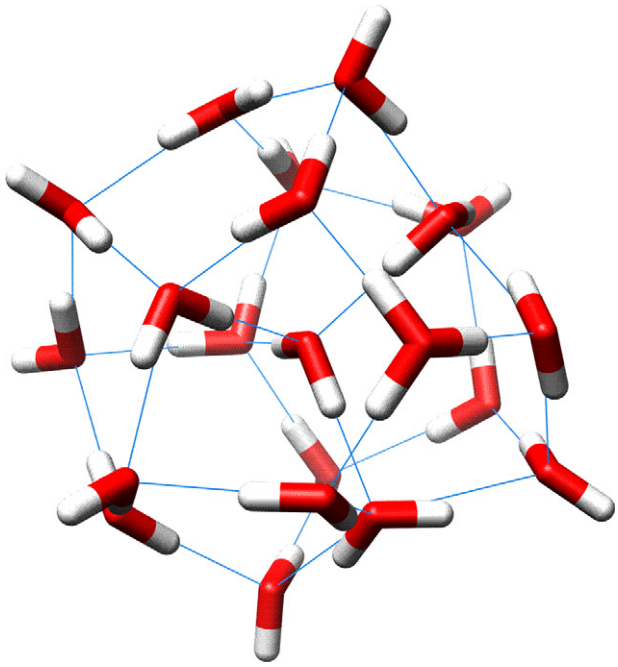

Fig. 1. An energy minimized model of the $[H(H_2O)_{21}]^+$ ion [15], a distorted dodecahedral cage in which each edge is a hydrogen bond. Note the 10 "dangling" O–H bonds (the dodecahedron has 20 vertices and 30 edges). The interior of the cage is occupied by a water molecule, clathrate-fashion; 1 of the 21 water molecules is protonated to form a hydronium ion.

hydronium ion [26]. Many Monte Carlo simulations and ab initio calculations have suggested that the hydronium ion is located on the surface of the cage [18,27,28] while others suggest that the hydronium ion is found in the centre of the cage [20,23,29,30]. More recent computational studies suggest that there is in fact a water molecule within the cage and the hydronium ion is found on the surface of the cage [6,19]. A similar clathrate-like structure is proposed for the $[H(H_2O)_{28}]^+$ cluster [6].

Wu et al. [6] studied the stability of $[H(H_2O)_{21}]^+$ under a variety of conditions. The authors used a continuous corona-discharge ion source to generate the clusters and performed the experiments in a vibrational predissociation ion trap tandem mass spectrometer with a pulsed infrared laser. Mass spectra showed that even at different backing pressures, anomalous intensities between the $n = 21$ and 22 clusters were observed. At higher backing pressures (340 Torr and 200 Torr) the $[H(H_2O)_{21}]^+$ cluster is the most intense peak in the spectrum and when compared to the dissociation fraction, it was observed that this cluster has significantly smaller dissociation rates than the $n = 20$ and 22 clusters. In order to present evidence for a distorted pentagonal dodecahedral cage the authors compared their results from vibrational predissociation spectroscopy with Monte Carlo simulations and density functional theory calculations. The vibrational predissociation spectrum of $[H(H_2O)_{21}]^+$ showed a single feature suggesting a three-coordinated water cluster. The results support the distorted pentagonal dodecahedral cage structure. Although these magic clusters have been studied at length with mass spectrometric, computational and spectroscopic methods, few have performed MS/MS studies to determine if larger clusters preferentially fragment to these magic clusters. Stace and Moore [31] generated water clusters using a pulsed molecular beam, which was then ionized by electron impact and dissociation fractions monitored by mass spectrometry. They measured dissociation fractions of $[H(H_2O)_n]^+$ and $[D(D_2O)_n]^+$, with n ranging from 5 to 26. Although they did not see any anomalies for the $n = 21$ cluster, they did find that the dissociation of $n = 22$ mer is much faster than the other clusters. Echt et al. [10] generated and studied $[H(H_2O)_{21}]^+$ clusters using electron impact ionization time-of-flight (TOF) mass spectrometry. The TOF spectra shows that after a time delay, anomalous intensities for the $[H(H_2O)_{21}]^+$ and $[H(H_2O)_{28}]^+$ clusters are evident. The authors varied the positive potential barrier applied in front of the detector and monitored the intensity of various cluster ions in order to study the amount of decomposition occurring in the drift tube of the TOF mass analyzer. They determined that while only 27% of the $[H(H_2O)_{21}]^+$ cluster decomposed, almost twice as much, about 50%, of the $[H(H_2O)_{22}]^+$ ion decomposed under the same conditions. Magnera et al. [32] calculated the proton hydration energies for clusters with 1–28 water molecules. Clusters were generated by fast-atom bombardment of ice and binding energies were subsequently studied using collision-induced dissociation (CID) mass spectrometry. It was determined that for cluster sizes $n \leq 9$ the binding energy decreases significantly but starts to increases slowly for $n > 9$. $[H(H_2O)_{21}]^+$ was found to bind about 2 kcal/mol more strongly than its neighbouring clusters due to its high stability. Schindler et al. [33] used an FTICR-MS and selected the $[H(H_2O)_{58}]^+$ water cluster for fragmentation. They noted that this cluster fragmented to form clusters of $n = 57$–51 but clusters $n = 55$ and 53 had particularly long lifetimes. While they did not fragment this large cluster further to study the production of smaller clusters, they showed that the $n = 21$ cluster had a longer lifetime than other clusters. The majority of fragmentation experiments in this field has been focussed on determining the dissociation fraction of various clusters and simply show that cluster only slightly larger than the magic cluster ($n = 21$ and 23) are less stable which is facilitated by the especially stable magic cluster and that $[H(H_2O)_{21}]^+$ cluster decomposes much more slowly than its neighbouring clusters.

Until now, no work has been done to determine if the fragmentation of large clusters will also provide evidence for the unusual stability of the $n = 21$ cluster. We have previously reported fragmentation studies of large triply charged lanthanide and methylated guanidinium water clusters [34,35]. Herein we use the same method and report the energy-dependent electrospray ionization tandem mass spectrometric (EDESI–MS/MS) analysis of $[H(H_2O)_n]^+$ where $n = 26$–76. Clusters larger than $[H(H_2O)_{21}]^+$ are mass selected for collision-induced dissociation in the argon-filled collision cell of the mass spectrometer. The collision voltage is increased and the intensities and distributions of the product ions are monitored. As the collision energy is increased the sequential loss of water molecules is observed:

$$[H(H_2O)_n]^+ + Ar \rightarrow [H(H_2O)_{n-1}]^+ + H_2O + Ar$$

$$[H(H_2O)_{n-1}]^+ + Ar \rightarrow [H(H_2O)_{n-2}]^+ + H_2O + Ar, \text{etc.}$$

The CID experiment is conducted under multiple-collision conditions, with product ions formed by dissociation of the selected precursor ion being further activated by subsequent collisions. Such conditions allow much greater total energy deposition, with the trade-off that activation is relatively slow (microseconds) and hence rearrangement can occur prior to fragmentation [36]. However, rearrangement of the water molecules in the droplet does not affect the conclusions we draw, since only in the case of the $n = 21$ cluster do we make assumptions about structure.

We report that all the precursor clusters studied (with as many as 76 water molecules) show strong evidence for an extended lifetime for the $[H(H_2O)_{21}]^+$ cluster. For each cluster size, a large amount of data is produced. EDESI–MS/MS [37–39] is used to simplify the presentation of the data as it allows it to be condensed and presented in a practical manner.

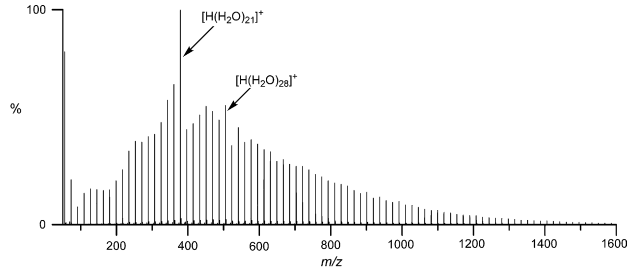

Fig. 2. Electrospray ionization mass spectrum of protonated water clusters. The $[H(H_2O)_{21}]^+$ cluster is "magic" due to its unusually high stability, also true but to a markedly lesser extent for $[H(H_2O)_{28}]^+$.

2. Experimental

All experiments were run on an unmodified Micromass Q-T of *micro*™ mass spectrometer at a capillary voltage of 2900 V and an ion energy of 1.0 V. Water clusters were generated by injecting 0.05% trifluoroacetic acid into the mass spectrometer at a rate of 50 μL/min. The cone voltage was maximized to 200 V and the source and desolvation temperatures were set to 60 °C and 20 °C, respectively. The cone gas was turned off and the desolvation gas flow rate was 250 L/h. The formation of water clusters was little affected by other parameters in the normal working range.

EDESI experiments were carried out by performing MS/MS on a selected peak and increasing the collision voltage in 1 V increments from 2 V until the spectrum was dominated by $[H(H_2O)_3]^+$. This final collision voltage depended on the size of cluster chosen for fragmentation. EDESI experiments were performed on $[H(H_2O)_n]^+$ (n = 26, 31, 36, 41, 46, 51, 56, 61, 66, 71 and 76). Spectra were collected for 3 s at each collision voltage.

3. Results and discussion

Protonated water clusters can be generated readily with ESI–MS by using high flow rates and low temperatures, under "cold-flooding" conditions. As previously reported, the peak corresponding to the $[H(H_2O)_{21}]^+$ cluster is observed to have much higher intensity than its neighbouring peaks. Not only does it have the greatest intensity but also we observe that the overall distribution peaks around this cluster size (Fig. 2). This however has more to do with the instrument and the conditions than anything else as other studies show somewhat different overall distributions of water clusters [3,5,6]. It has been reported that this distribution changes depending on the temperature of the solution, the temperature in the gas phase and the humidity in the air [4]. In all studies, the n = 21 peak is significantly larger than its immediate neighbours. The disruption in distribution is observed for a range of clusters. The n = 21 cluster has an anomalously large intensity while the intensity of its nearby clusters, n = 22, 23, and possibly 24, decreases and facilitates the formation of the n = 21 cluster. The "weak" maximum of the n = 28 peak can also be observed in Fig. 2. This peak is emphasized by the particularly low intensity of the neighbouring n = 29 cluster which is dissociates much faster to generate the n = 28 cluster.

Highly solvated protonated water clusters (n = 26–76; we started at a value of 21 + 5 and proceeded in +5 intervals; this choice was essentially arbitrary) were mass selected for EDESI–MS experiments. In each experiment, the selected peak preferentially fragmented to the $[H(H_2O)_{21}]^+$ cluster, as can be seen in Fig. 3 for the example of $[H(H_2O)_{66}]^+$. The contour plot shows the successive loss of water molecules as the collision voltage is increased. A summation plot is presented above the contour map. This plot is generated by summing all the product ion data generated from the EDESI–MS/MS experiment. The most intense peak in this summed plot corresponds to $[H(H_2O)_{21}]^+$. Again this peak is significantly larger than it neighbouring peaks and a decrease in intensity of clusters with n = 22–23 is observed. This decrease could be explained by the instability of these clusters previously observed [10,31]. Although the $[H(H_2O)_{28}]^+$ does not appear to have a particularly special intensity in the summation plot, it does have a significantly larger intensity than the $[H(H_2O)_{29}]^+$cluster.

A more dramatic depiction of the special intensity of the $[H(H_2O)_{21}]^+$ cluster ion in this experiment can be obtained by representing the intensity data as a 3D surface (Fig. 4). In this 3D plot, a fairly steady intensity of water clusters is observed with the exception of the anomalously strong peak at m/z 379.24 corresponding to the $[H(H_2O)_{21}]^+$ cluster. What appears as a fairly uniform "wave" of ions is interrupted by a distinct spike in intensity.

Note also that this peak is broader than all other peaks in the plot indicating that this cluster is a predominant feature at more than one collision voltages. In fact, the $[H(H_2O)_{21}]^+$ cluster is observed to dominate the MS/MS spectrum at lower collision voltages than expected and maintains its strong intensity for a larger range of collision voltages than other clusters. Typically a single cluster will be the base peak in the MS/MS spectra only for one or two different values of the collision voltage. The magic $[H(H_2O)_{21}]^+$ cluster dominates the MS/MS spectra (is the base peak) for more than 15 consecutive collision voltage settings. As seen in Fig. 3, the intensities of cluster generated at higher collision voltages decreases steadily as the collision voltage increases, with the exception of $[H(H_2O)_{21}]^+$. The general decrease is accounted for by the fact that the ion intensity of the originally selected ion, $[H(H_2O)_n]^+$, is now distributed across a large number of product ions.

A peak that is slightly higher than its neighbouring clusters can also be seen for the $[H(H_2O)_{28}]^+$ cluster and an anomalously small

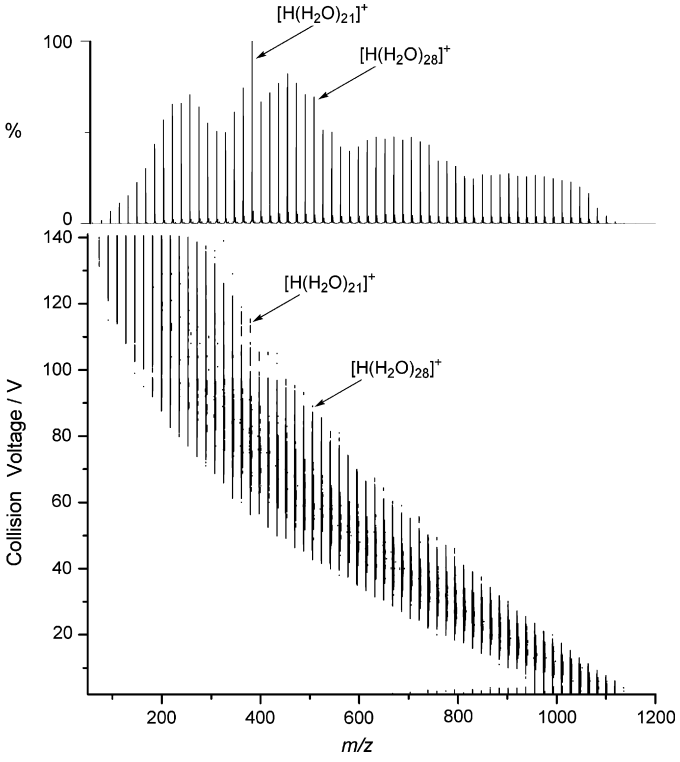

Fig. 3. EDESI–MS/MS plot of $[H(H_2O)_{66}]^+$. The fragmentation energy increases vertically on the contour plot. The top spectrum is a summation of all 139 spectra (collision voltage = 2–140) used to generate the contour plot.

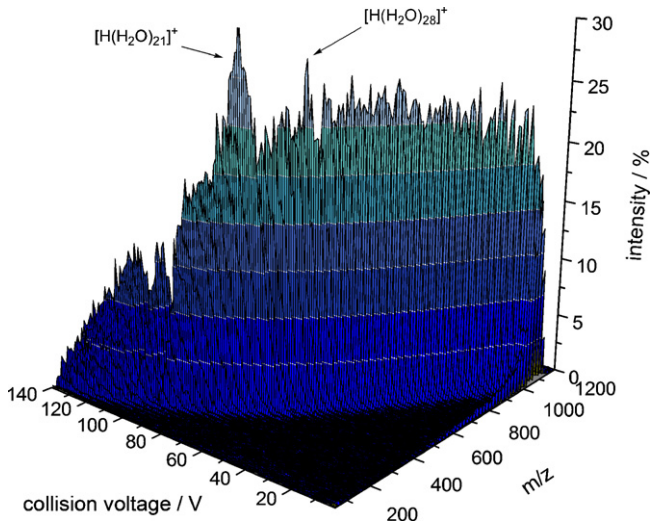

Fig. 4. EDESI–MS/MS 3D plot of $[H(H_2O)_{66}]^+$. The stability of the $[H(H_2O)_{21}]^+$ is also observed through CID as larger clusters preferentially fragment to this species.

peak is observed for the $[H(H_2O)_{29}]^+$ cluster indicating the preferential formation of the magic $[H(H_2O)_{28}]^+$ cluster. This species however did not to have a prolonged existence over a large range of collision voltages.

EDESI data from the fragmentation of clusters containing 26–76 water molecules each show the $[H(H_2O)_{21}]^+$ cluster having an anomalous intensity (see supporting information). In all cases, the successive fragmentation of a larger water cluster eventually leads to the preferential generation of the $[H(H_2O)_{21}]^+$ magic water cluster.

To demonstrate the large range of water clusters that fragment to preferentially generate the $[H(H_2O)_{21}]^+$ cluster, an EDESI–MS/MS plot of the much smaller $[H(H_2O)_{36}]^+$ cluster is presented in Fig. 5. Again, the most intense peak in the summation plot is the $[H(H_2O)_{21}]^+$ cluster which has a much larger intensity than its neighbouring clusters. Similarly, the $[H(H_2O)_{28}]^+$ cluster is not especially intense, but is much more abundant than the $[H(H_2O)_{29}]^+$ cluster.

One unexpected feature of all the EDESI–MS/MS spectra is the consistent appearance of broad intensity maxima centered at about the 13-mer, 25-mer and 36-mer clusters, and a distinct minimum at the 32-mer. These features are quite different from the "spike" apparent for the 21-mer, or the more subtle increased intensity of the 28-mer; the increased intensity is not at the expense of the

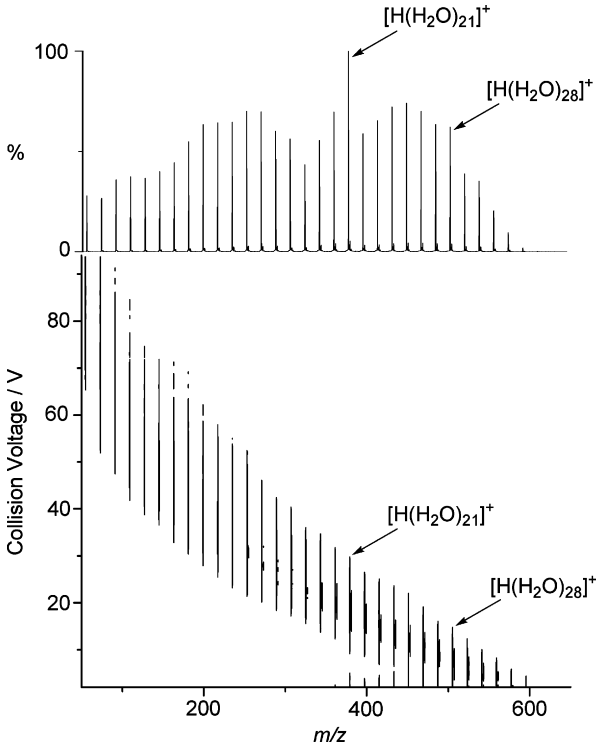

Fig. 5. EDESI–MS/MS plot of $[H(H_2O)_{36}]^+$. The fragmentation energy increases vertically on the contour plot. The top spectrum is a summation of all 92 spectra (collision voltage = 2–94) used to generate the contour plot.

neighbouring peaks, it instead manifests itself as the superposition of an approximately sinusoidal wave upon the background intensity. Interestingly, the "wave" has maxima every 12–13 water molecules, and the undulation can be seen to continue out farther for the larger clusters. Fig. 6 shows a composite spectrum, compiled from the summation plots for every experiment conducted.

Because these features are so consistent from spectrum to spectrum, regardless of the initial cluster size selected, we suspect these features to be real – i.e., indicating an extended lifetime for those clusters with higher intensity – and not some strange artefact of the CID experiment. The same pattern is weakly present in the original ensemble of clusters (Fig. 2). We are unsure of the significance of this observation, as theoretical studies of the energies of global minima of protonated water clusters (to the 20-mer) reveal a very consistent energy change as each water molecule is added, with no notable discontinuities [22]. Interestingly, experimental

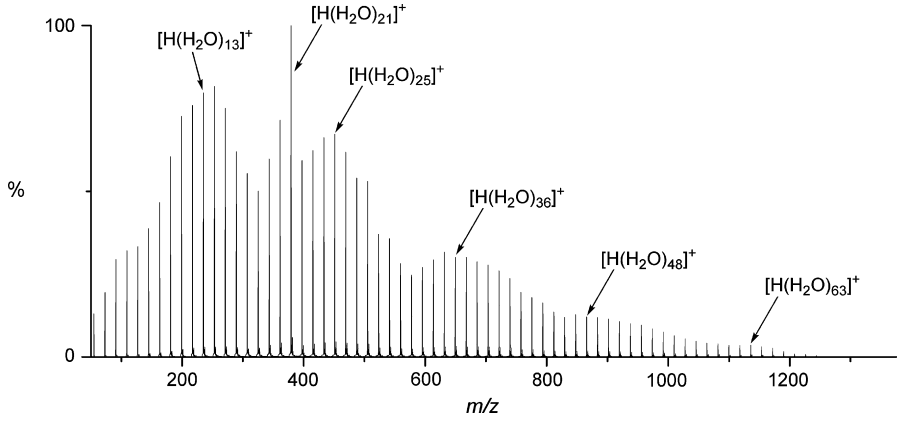

Fig. 6. Composite of summation plots of each experiment completed.

and theoretical studies of some rare gas clusters indicate particularly stable icosahedral structures for the 13-mer among others [40–42]. However, the mass spectra of these species display sharply higher intensities for the magic numbers, not the broad maxima seen here. It seems unlikely that the pattern observed in Fig. 6 is due to the same icosahedral structure responsible for the stability of the rare gas clusters.

These EDESI experiments demonstrate a novel approach to demonstrate that $[H(H_2O)_{21}]^+$ does indeed have much higher stability than not only its neighbouring clusters, but also all other protonated water clusters less than $[H(H_2O)_{76}]^+$. We also reveal the existence of some new, subtle stability trends in protonated water clusters that appear as broad maxima every 12–13 water molecules, though we provide no explanation as yet for this phenomenon.

Acknowledgments

J.S.M. and F.H. both thank the Natural Sciences and Engineering Research Council (NSERC) of Canada, the Canada Foundation for Innovation (CFI) and the British Columbia Knowledge Development Fund (BCKDF), and the University of Victoria for instrumentation and operational funding. K.M. thanks the University of Victoria for a graduate fellowship and the Nora and Mark Degoutiere Memorial Scholarship. We thank Ken Jordan of the University of Pittsburgh for providing the structural model of the magic water cluster.

Appendix A. Supplementary data

Supplementary data associated with this article can be found, in the online version, at doi:10.1016/j.ijms.2008.10.001.

References

[1] P. Ball, Water as an active constituent in cell biology, Chem. Rev. 108 (2008) 74–108.
[2] F. Dong, S. Heinbuch, J.J. Rocca, E.R. Bernstein, Dynamics and fragmentation of van der Waals clusters: $(H_2O)_n$, $(CH_3OH)_n$, and $(NH_3)_n$ upon ionization by a 26.5 eV soft X-ray laser, J. Chem. Phys. 124 (2006) 224319.
[3] D.W. Ledman, R.O. Fox, Water cluster calibration reduces mass error in electrospray ionization mass spectrometry of proteins, J. Am. Soc. Mass Spectrom. 8 (1997) 1158–1164.
[4] S.-S. Lin, Detection of large water clusters by a low rf [radio frequency] quadrupole mass filter, Rev. Sci. Instr. 44 (1973) 516–517.
[5] X. Yang, A.W. Castleman Jr., Large protonated water clusters $H^+(H_2O)_n$ ($1 \leq n > 60$): the production and reactivity of clathrate-like structures under thermal conditions, J. Am. Chem. Soc. 111 (1989) 6845–6846.
[6] C.-C. Wu, C.-K. Lin, H.-C. Chang, J.-C. Jiang, J.-L. Kuo, M.L. Klein, Protonated clathrate cages enclosing neutral water molecules: $H^+(H_2O)_{21}$ and $H^+(H_2O)_{28}$, J. Chem. Phys. 122 (2005) 074315.
[7] M. Tsuchiya, T. Tashiro, A. Shigihara, Water clusters in gas phases studied by liquid ionization mass spectrometry, J. Mass Spectrom. Soc. Jpn. 52 (2004) 1–12.
[8] G. Hulthe, G. Stenhagen, O. Wennerstroem, C.-H. Ottosson, Water clusters studied by electrospray mass spectrometry, J. Chromatogr. A 777 (1997) 155–165.
[9] P.P. Radi, P. Beaud, D. Franzke, H.M. Frey, T. Gerber, B. Mischler, A.P. Tzannis, Femtosecond photoionization of $(H_2O)_n$ and $(D_2O)_n$ clusters, J. Chem. Phys. 111 (1999) 512–518.
[10] O. Echt, D. Kreisle, M. Knapp, E. Recknagel, Evolution of "magic numbers" in mass spectra of water clusters, Chem. Phys. Lett. 108 (1984) 401–407.
[11] S.Y. Huang, C.D. Huang, B.T. Chang, C.T. Yeh, Chemical activity of palladium clusters: sorption of hydrogen, J. Phys. Chem. B 110 (2006) 21783–21787.
[12] Z. Shi, J.V. Ford, S. Wei, A.W. Castleman Jr., Water clusters: contributions of binding energy and entropy to stability, J. Chem. Phys. 99 (1993) 8009–8015.
[13] K. Mori, D. Asakawa, J. Sunner, K. Hiraoka, Electrospray droplet impact/secondary ion mass spectrometry: cluster ion formation, Rapid Commun. Mass Spectrom. 20 (2006) 2596–2602.
[14] J.C. Searcy, J.B. Fenn, Clustering of water on hydrated protons in a supersonic free jet expansion, J. Chem. Phys. 61 (1974) 5282–5288.
[15] S.J. Park, D.M. Shin, S. Sakamoto, K. Yamaguchi, Y.K. Chung, M.S. Lah, J.I. Hong, Dynamic equilibrium between a supramolecular capsule and bowl generated by inter- and intramolecular metal clipping, Chem. Eur. J. 11 (2004) 235–241.
[16] J.M. Headrick, E.G. Diken, R.S. Walters, N.I. Hammer, R.A. Christie, J. Cui, E.M. Myshakin, M.A. Duncan, M.A. Johnson, K.D. Jordan, Spectral signatures of hydrated proton vibrations in water clusters, Science 308 (2005) 1765–1769.
[17] M. Miyazaki, A. Fujii, T. Ebata, N. Mikami, Infrared spectroscopic evidence for protonated water clusters forming nanoscale cages, Science 304 (2004) 1134–1137.
[18] A. Khan, Ab initio studies of $(H_2O)_{20}H^+$ and $(H_2O)_{21}H^+$ prismic, fused cubic and dodecahedral clusters: can H_3O^+ ion remain in cage cavity? Chem. Phys. Lett. 319 (2000) 440–450.
[19] S.S. Iyengar, M.K. Petersen, T.J.F. Day, C.J. Burnham, V.E. Teige, G.A. Voth, The properties of ion–water clusters. I. The protonated 21-water cluster, J. Chem. Phys. 123 (2005) 084309.
[20] H. Shinohara, U. Nagashima, H. Tanaka, N. Nishi, Magic numbers for water–ammonia binary clusters: enhanced stability of ion clathrate structures, J. Chem. Phys. 83 (1985) 4183–4192.
[21] D.J. Wales, M.P. Hodges, Global minima of water clusters $(H_2O)_n$, $n \leq 21$, described by an empirical potential, Chem. Phys. Lett. 286 (1998) 65–72.
[22] M.P. Hodges, D.J. Wales, Global minima of protonated water clusters, Chem. Phys. Lett. 324 (2000) 279–288.
[23] M. Svanberg, J.B.C. Pettersson, Structure and thermodynamics of $H^+(H_2O)_n$ ($n = 9, 21, 40$) clusters between 0 and 300 K – a Monte Carlo study, J. Phys. Chem. A 102 (1998) 1865–1872.
[24] C.C. Wu, C.K. Lin, H.C. Chang, J.C. Jiang, J.L. Kuo, M.L. Klein, Protonated clathrate cages enclosing neutral water molecules: $H^+(H_2O)_{(21)}$ and $H^+(H_2O)^{(28)}$, J. Chem. Phys. 122 (2005).
[25] E. Brodskaya, A.P. Lyubartsev, A. Laaksonen, Investigation of water clusters containing OH^- and H_3O^+ ions in atmospheric conditions. a molecular dynamics simulation study, J. Phys. Chem. B 106 (2002) 6479–6487.
[26] T.S. Zwier, The structure of protonated water clusters, Science 304 (2004) 1119–1120.
[27] P.M. Holland, A.W. Castleman Jr., A model for the formation and stabilization of charged water clathrates, J. Chem. Phys. 72 (1980) 5984–5990.
[28] R. Kelterbaum, E. Kochanski, Behavior and evolution of the first 28 protonated hydrates from Monte Carlo studies, J. Phys. Chem. 99 (1995) 12493–12500.
[29] R.E. Kozack, P.C. Jordan, Structure of hydrogen ion hydrate $(H^+(H_2O)_n)$ clusters near the magic number $n = 21$, J. Chem. Phys. 99 (1993) 2978–2984.
[30] K. Laasonen, M.L. Klein, Structural study of $(H_2O)_{20}$ and $(H_2O)_{21}H^+$ using density functional methods, J. Phys. Chem. 98 (1994) 10079–10083.
[31] A.J. Stace, C. Moore, A correlation between structure and reactivity in ion clusters, Chem. Phys. Lett. 96 (1983) 80–84.
[32] T.F. Magnera, D.E. David, J. Michl, The first twenty-eight gas-phase proton hydration energies, Chem. Phys. Lett. 182 (1991) 363–370.
[33] T. Schindler, C. Berg, G. Niedner-Schatteburg, V.E. Bondybey, Protonated water clusters and their black body radiation induced fragmentation, Chem. Phys. Lett. 250 (1996) 301–308.
[34] K. McQuinn, F. Hof, J.S. McIndoe, Direct observation of ion evaporation from a triply charged nanodroplet, Chem. Commun. (2007) 4099–4101.
[35] K. McQuinn, J.S. McIndoe, F. Hof, Insights into post-translational methylation of arginine from studies of guanidinium–water nanodroplets, Chem. Eur. J. 14 (2008) 6483–6489.
[36] S.A. McLuckey, Principles of collisional activation in analytical mass spectrometry, J. Am. Soc. Mass Spectrom. 3 (1992) 599–614.
[37] C.P.G. Butcher, B.F.G. Johnson, J.S. McIndoe, X. Yang, X.-B. Wang, L.-S. Wang, Collision-induced dissociation and photodetachment of singly and doubly charged anionic polynuclear transition metal carbonyl clusters: $Ru_3Co(CO)_{13}^-$, $Ru_6C(CO)_{16}^{2-}$, and $Ru_6(CO)_{18}^{2-}$, J. Chem. Phys. 116 (2002) 6560–6566.
[38] P.J. Dyson, A.K. Hearley, B.F.G. Johnson, J.S. McIndoe, P.R.R. Langridge-Smith, C. Whyte, Combining energy-dependent electrospray ionisation with tandem mass spectrometry for the analysis of inorganic compounds, Rapid Commun. Mass Spectrom. 15 (2001) 895–897.
[39] P.J. Dyson, B.F.G. Johnson, J.S. McIndoe, P.R.R. Langridge-Smith, Energy-dependent electrospray ionization mass spectrometry: applications in transition metal carbonyl chemistry, Rapid Commun. Mass Spectrom. 14 (2000) 311–313.
[40] W. Miehle, O. Kandler, T. Leisner, O. Echt, Mass-spectrometric evidence for icosahedral structure in large rare-gas clusters – Ar, Kr, Xe, J. Chem. Phys. 91 (1989) 5940–5952.
[41] I.A. Harris, R.S. Kidwell, J.A. Northby, Structure of charged argon clusters formed in a free jet expansion, Phys. Rev. Lett. 53 (1984) 2390–2393.
[42] J.D. Honeycutt, H.C. Andersen, Molecular-dynamics study of melting and freezing of small Lennard-Jones clusters, J. Phys. Chem. 91 (1987) 4950–4963.